

Validated Dark Current Spectroscopy on a per-pixel basis in CMOS image sensors

Eric A. G. Webster^{1*}, Robert Nicol², Lindsay Grant², David Renshaw¹

1. School of Engineering & Electronics, The University of Edinburgh, King's Buildings, Mayfield Road, Edinburgh, United Kingdom, EH9 3JL

2. STMicroelectronics (R&D) Ltd., 33 Pinkhill, Edinburgh, United Kingdom, EH12 7BF

*. **Contact:** 38 Crompton Avenue, Cathcart, Glasgow, United Kingdom, G44 5TH

Email: eagwebster@googlemail.com **Tel:** +447717671003

I. ABSTRACT

A per-pixel Dark Current Spectroscopy technique for characterising deep-level traps in CMOS imagers is presented. The short integration time (10–15ms) experimental method used to obtain accurate results is described. The activation energies are correctly obtained for molybdenum ($\approx 0.3\text{eV}$) and phosphorus-vacancy (E-centre) ($\approx 0.44\text{eV}$) trap levels in silicon. These match published activation energy data. The Meyer-Neldel Relationship (MNR) was observed between the calculated pre-exponential factor and activation energy. The MNR yields an Isokinetic temperature of ≈ 293 Kelvin and this is used to calculate the total capture cross-section for molybdenum as $\approx 1.5 \times 10^{-16}\text{cm}^2$ and for the E-centre as $\approx 2.5 \times 10^{-16}\text{cm}^2$. Evidence is presented for electric field enhanced emission and Poole-Frenkel barrier force lowering of E-centre defects in the pinning implant regions.

II. INTRODUCTION

Dark Current Spectroscopy (DCS) was developed in 1992 as a method for determining the trap energy levels of contaminants in CCDs from the analysis of the dark current-temperature relationship [1]. The large full well capacities of CCDs [2] are ideal for the study of dark current as heavy metal traps can very rapidly produce thousands of free carriers at high temperatures. The relatively small full wells of CMOS imagers make it difficult to obtain accurate and representative dark current data.

This paper presents a method for obtaining activation energies and capture cross-sections for traps in CMOS image sensors using DCS techniques. The experimental procedure used is described first and an example output given. This is followed by a discussion of the observed Meyer-Neldel Relationship (MNR). The MNR is then used to present evidence for electric field enhanced emission and Poole-Frenkel barrier force lowering of E-centre defects in the pinning implant regions. The capture cross-section calculation is then detailed.

III. EXPERIMENTAL METHOD

A three megapixel CMOS image sensor intentionally contaminated with molybdenum was placed in an oven and the temperature swept in 5K increments from 293K to 363K. Ten image frames were sampled and averaged with the transfer gate enabled and then with the transfer gate disabled at each temperature. The latter was then subtracted from the former to cancel fixed pattern noise sources. Integration times between 10 and 15ms were chosen to minimise the number of saturated pixels at 363K. It was found

from numerous experiments that if longer integration times were used the calculated activation energy was incorrect.

The averaged and subtracted image frames were then imported into MATLAB and the generation rate in electrons per second calculated at each temperature for each photodiode. An Arrhenius plot was created for each photodiode to calculate the activation energy, E_a , and pre-exponential frequency factor, A , of the individual pixels, using the Arrhenius equation:

$$k = A \exp\left(-\frac{E_a}{k_B T}\right) \quad 1$$

where k is the generation rate in electrons per second, k_B Boltzmann's constant, and T the temperature in Kelvin. The analysis produced two matrices of coefficients corresponding to A and E_a for each photodiode.

IV. RESULTS

The majority of the dark noise was due to charge injection from the transfer gate because of the short integration times used for measurement. This resulted in a large number of uncontaminated photodiodes with activation energies between 0 and 0.1eV, and not of the order of the band gap. These were filtered out of the activation energy matrix to reveal the photodiodes affected by deep-level states, and a histogram created (Fig. 1).

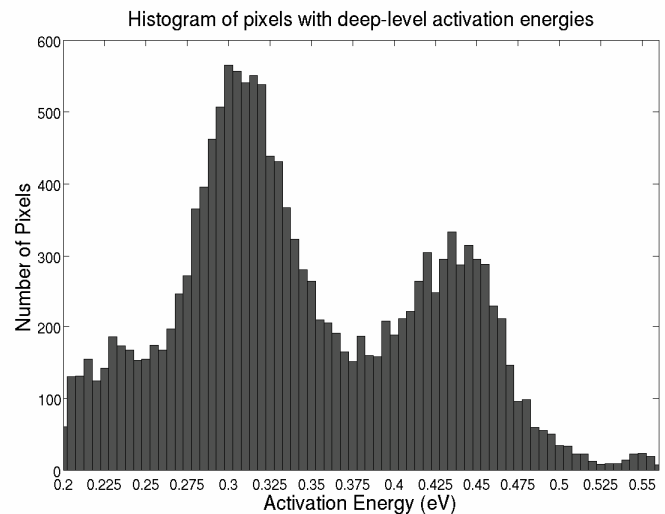


Fig. 1: Density of deep-level defect states for image sensor contaminated with molybdenum. The peak at 0.3eV is due to molybdenum and the 0.44eV peak due to the E-centre.

Fig. 1 illustrates the results from the Dark Current Spectroscopy analysis on a molybdenum contaminated sensor. Two peaks are evident: one at $\approx 0.3\text{eV}$ and one at $\approx 0.44\text{eV}$. The 0.3eV peak is in the correct position to be attributed to the molybdenum defect level [3-6]. The literature associates the 0.44eV defect level with a Phosphorus-Vacancy complex, often termed the 'E-Centre,' which is a by-product of modern fabrication processes, such as plasma etching and ion-implantation [2]. The E-centre is a multi-atom defect construct created when two vacancies in the silicon lattice combine with a phosphorus or arsenic atom [2]. The accepted Shockley-Read-Hall recombination model [7] could not be used to calculate the capture cross-section of the traps as it yielded an activation energy dependence due to the Meyer-Neldel Relationship.

V. THE MEYER-NELDEL RELATIONSHIP

The Meyer-Neldel Relationship was first discovered in 1937 by Von Wilfried Meyer and Hans Neldel [8]. This Relationship has also been recently observed in the behaviour of dark current in CCDs [9]. It appears from the literature that there is no widely accepted explanation for the existence of the Relationship [8-10]. This Relationship is observed between the activation energy and pre-exponential factor calculated for each photodiode during the performed per-pixel dark current analysis. The mathematical statement of the Relationship is [10]:

$$A = A_0 \exp\left(\frac{E_a}{E_{mn}}\right) \quad 2$$

where A is the pre-exponential factor in the Arrhenius equation (1), E_a is the activation energy, and E_{mn} is the Meyer-Neldel energy. A_0 is termed the 'true pre-exponential factor' as it agrees with theoretical calculations [8]. The Meyer-Neldel energy can be found by plotting the natural log of the pre-exponential factor against activation energy, for each photodiode, and performing a straight line fit (Fig. 2).

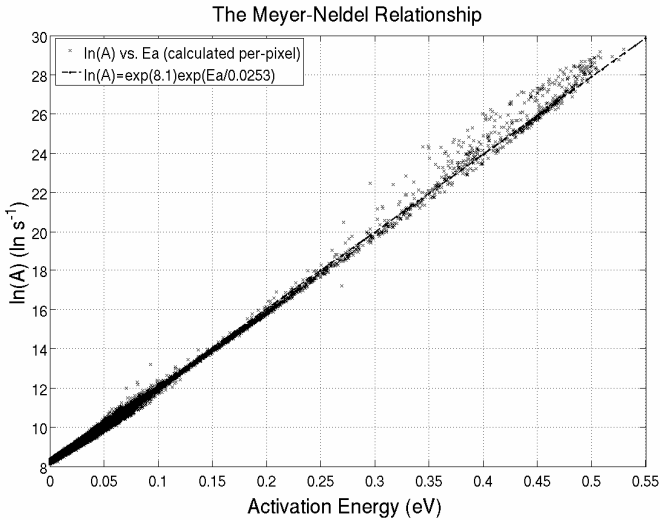


Fig. 2: The Meyer-Neldel Relationship between E_a and $\ln(A)$.

The gradient of the best fit line in Fig. 2 is equal to E_{mn} , and is approximately 0.0253eV . This result is consistent with previous dark current studies performed with CCDs [9]. Fig. 2 plots the results of fifteen measured temperatures, where each data point is itself comprised of a ten-frame average, for the three million individual photodiodes in the array.

To produce a modified Arrhenius equation that incorporates the Meyer-Neldel Relationship, Equation 2 is substituted into Equation 1 and simplified:

$$k = A_0 \exp\left(-E_a\left(\frac{1}{k_B T} - \frac{1}{E_{mn}}\right)\right) \quad 3$$

When a specific temperature is inserted into Equation 3 the value contained in the exponent is zero and therefore the generation rate only depends on A_0 . This is known as the Isokinetic temperature and, according to the gradient of Fig. 2 (0.0253eV), is approximately 293 Kelvin. The value of A_0 can be determined by rearranging Equation 2:

$$A_0 = \frac{A}{\exp\left(\frac{E_a}{E_{mn}}\right)} \quad 4$$

The Meyer-Neldel Relationship exhibited in Fig. 2 can be corrected using Equation 4 to yield A_0 for each photodiode. The trend in the scatter plot of A_0 against activation energy is observed to be relatively flat (Fig. 3).

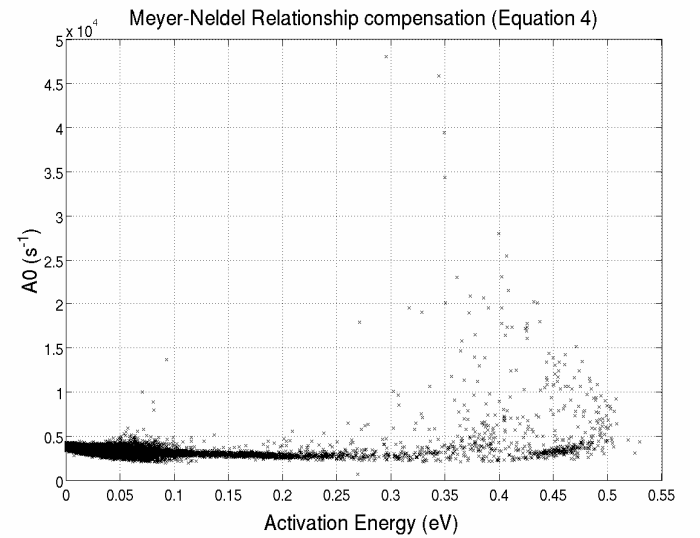


Fig. 3: Scatter plot of MNR-corrected pre-exponential factors (A_0) against activation energy.

VI. ELECTRIC FIELD ENHANCED DARK CURRENT GENERATION

As can be observed from Fig. 3, most photodiodes exhibit approximately the same value of A_0 after compensating for the Meyer-Neldel Relationship. The interesting section of Fig. 3 is data points corresponding to energies between 0.3 and 0.5eV , for which there is a vertical relationship and a left skew. This behaviour is consistent with the assumption that some 0.44eV E-centre defects exist within the depletion regions created by the p -isolation. These defects will thus exist in regions of high local electric field and will exhibit enhanced emission rates. This correlates strongly with the large pre-exponential factors exhibited by some photodiodes with 0.44eV activation energy and previous studies [11].

The left skew is thought to be due to the Poole-Frenkel barrier force-lowering effect [12] which is also caused by the high local electric field. Using an expression for the one-dimensional emission enhancement factor, Γ , due to an electric field [11], an approximate calculation appears to match the observed relationship in Fig. 3:

$$\Gamma = \frac{e_1}{e_0} = \exp\left(-\frac{\Delta E}{k_B T}\right) \quad 5$$

where the enhanced emission rate e_l , in electrons per second, is taken as one of the outliers in Fig. 3 at approximately 2.4×10^4 and the normal emission rate e_0 taken as approximately 2.5×10^3 from the main distribution. The energy shift, ΔE , is then approximately -0.05eV which correlates with the magnitude of the left skew observed in Fig. 3.

VII. CALCULATION OF CAPTURE CROSS-SECTION

The widely accepted method of calculating the capture cross-section of traps in semiconductors is the recombination model developed by Shockley, Read, and Hall [7], in the 1950s. The key assumption of the capture cross-section calculation presented here is that the generation rate is the MNR-corrected generation rate, A_0 , at the Isokinetic temperature (293K). When the value for A_0 is fed into the Shockley-Reid-Hall (SRH) [3], [7] recombination model, the calculated capture cross-section exhibits an activation energy dependence and, for molybdenum, produces results which are orders of magnitude larger than those quoted in the literature [5]. However, the equations for the individual emission rates of electrons and holes, $e_{n/p}$, that are used to derive the SRH recombination model are of the form (for emission):

$$e_{n/p} = \sigma_{n/p} v_{th,n/p} N_{c/v} \exp\left(-\frac{E_a}{k_B T}\right) \quad 6$$

where $\sigma_{n/p}$ is the capture cross-section for electrons or holes, $v_{th,n/p}$ is the thermal velocity for electrons or holes, $N_{c/v}$ is the effective density of states in the conduction or valence bands, and E_a is the trap activation energy. From the Meyer-Neldel Relationship, the temperature-independent cross-section can be calculated from A_0 and the result will not be distorted by the activation energy of the trap. At the Isokinetic temperature, the value in the exponent of Equation 6 becomes zero, due to Equation 3. Therefore, Equation 6 becomes:

$$e_{n/p} = \sigma_{n/p} v_{th,n/p} N_{c/v} \quad 7$$

From comparing Equation 3 to Equation 7 it appears that A_0 may contain the values of net emission rate and thermal velocity. This is because the coefficients in Equation 7 are used to represent the volume of space swept by a trap in unit time [7]. It is known that the rate of dark current generation is strongly dependent on the magnitude of the electric field in which the defect lies [11], as discussed earlier. Assuming this premise, and that the exact value of the thermal velocity in each photodiode is unknown, the value of A_0 calculated for each photodiode will include the net generation rate and the local thermal velocity and these variables cannot be separated. The inseparability of these coefficients is indicated in Equation 8, and thereafter, by square brackets:

$$A_0 = \left[\frac{e_{p/n}}{v_{th,p/n}} \right] \quad 8$$

Substituting Equation 8 into Equation 7 and simplifying:

$$\left[\frac{e_{p/n}}{v_{th,p/n}} \right] = \sigma_{p/n} N_{v/c} \quad 9$$

However, one is now left with two inseparable equations as it cannot be known which side of the mid-band the trap exists. Due to the law of detailed balance [3], a conduction electron cannot be created without the subsequent creation of a hole in the valence band. This is a valid assumption as the short measurement time used in the experimental procedure is orders of magnitude greater than the uncertainty time. As can be seen from Equation 9, the

capture cross-section depends on the effective density of states in the conduction or valence bands. In multi-stage reactions, the overall rate of the reaction is limited by the rate of the slowest individual stage [13]. Conceptually, for the generation of dark current, this would be the creation of holes because the density of states is lower in the valence band. Therefore, it follows that the dark current generation rate will be limited by the number of states in the valence band. Dividing A_0 by the effective density of states in the valence band at 293K [3] yields total capture cross-sections which are of the correct order of magnitude:

$$\sigma_{p/n} = \sigma_0 = \frac{\left[\frac{e_{p/n}}{v_{th,p/n}} \right]}{N_{v/c}} = \frac{A_0}{N_{v(293K)}} \quad 10$$

Equation 10 was used on the data from the molybdenum contaminated sensor illustrated in Fig. 1. Fig. 4 illustrates the result as a scatter plot of capture cross-section against activation energy:

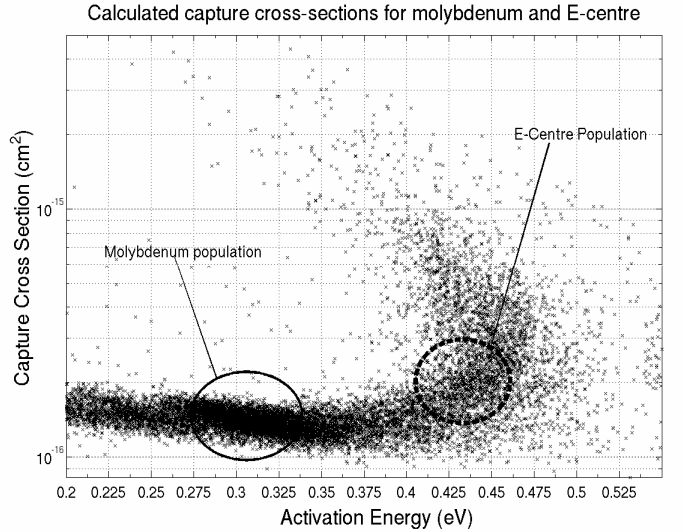


Fig. 4: Scatter plot of capture cross-section against activation energy for molybdenum (solid ellipse) and the E-centre (dashed circle).

The molybdenum population is indicated by the solid ellipse, and the E-centre by the dashed circle. A direct comparison can be made between the scatter plot in Fig. 4 and the histogram of Fig. 1. As previously discussed, the reason for the delocalisation of the E-centre's σ_0 is due to the high electric field altering the emission rate and the activation energy via the Poole-Frenkel effect [11], [12].

The total capture cross-section, σ_0 , for the 0.44eV defect ($\approx 2.5 \times 10^{-16} \text{cm}^2$) is larger than that calculated for molybdenum ($\approx 1.5 \times 10^{-16} \text{cm}^2$). Both calculated values correspond to published results from DLTS experiments [4], [14].

VIII. CONCLUSION

Dark Current Spectroscopy techniques have been shown to yield the correct activation energy for molybdenum and the E-centre in modern CMOS image sensors with small full wells. The crucial result is that short integration times in the range of 10-15ms must be used in order to obtain the correct activation energies. Also, creating a histogram of the activation energies calculated for each photodiode is an effective method of visualising the traps present in image sensors.

The Meyer-Neldel Relationship obtained between calculated activation energy and pre-exponential factor was used to present evidence for electric field enhanced dark current generation. A

large proportion of the generation rate enhanced defects were found to have activation energies of approximately 0.44eV. The emission enhancement factors and activation energies observed are consistent with these particular defects existing in the depletion regions created by the pinning implants in the active pixel structure. Additionally, the observed MNR was essential for calculating the capture cross-sections of each trap. The measurement and analysis technique presented could potentially be useful to the image sensor industry for diagnosing fabrication plant contamination.

IX. ACKNOWLEDGEMENT

The author would like to thank: ST Microelectronics for funding the MEng. project; R. Nicol & D. Renshaw for their help and support; S. Pellegrini & C. Sprought for experimental help; L. Grant & A. Holmes for technical help; and A. Adegbite for MATLAB help.

X. REFERENCES

- [1] W. C. McColgin, J. P. Lavine, J. Kyan, D. N. Nichols & C. V. Stancampiano: "Dark Current Quantization in CCD Image Sensors," *Eastman Kodak Company, Microelectronics Technology Division, Rochester, NY 14650-2019*.
- [2] J. R. Janesick: "Scientific Charge-Coupled Devices," The Society of Photo-Optical Instrumentation Engineers, 2001, ISBN: 0-8194-3698-4.
- [3] S. M. Sze: "Physics of Semiconductor Devices," *Second Edition*, John Wiley & Sons, 1981, ISBN: 0-471-09837-X, p. 21.
- [4] H. Pettersson, H. G. Grimmeiss, L. Tilly, K. Schmalz, K. Tittlebach, H. Kerkow: "Electrical and optical properties of molybdenum and tungsten related defects in silicon," *Semicond. Sci. Technol.* Volume 6, 1991, pp. 237 – 242.
- [5] M. Aoki, T. Itakura & N. Sasaki: "Mo Contamination in p/p+ Epitaxial Silicon Wafers," *Jpn. J. Appl. Phys.* Volume 34, 1995, pp. 712 – 714.
- [6] J. T. Borenstein, B. R. Bathey, J. P. Kalejs, J. I. Hanoka & N. O. Pearce: "Titanium- and Molybdenum-related levels in efg silicon," *Photovoltaic Specialists Conference*, 1991, Conference Record of the Twenty Second IEEE, pp. 1006 – 1009.
- [7] W. Shockley & W. T. Read, Jr.: "Statistics of the Recombinations of Holes and Electrons," *Phys. Rev.* Volume 87, Issue 5, 1952, pp. 835 – 842.
- [8] V. W. Meyer & H. Neldel: "Über die Beziehungen zwischen der Energiekonstanten ϵ und der Mengenkosten α in der Leitwert-Temperaturformel bei oxydischen Halbleitern," *Zeitschrift Für Technische Physik*, Volume 12, 1937, pp. 588 – 593.
- [9] R. Widenhorn, E. Bodegom & L. Mündermann: "Meyer-Neldel rule for dark current in charge-coupled devices," *Journal of Applied Physics*, Volume 89, Issue 12, 2001, pp. 8179.
- [10] E. Bodegom, R. Widenhorn, D. A. Iordache: "New Meyer-Neldel relations for the depletion and diffusion dark currents in some CCDs," *Semiconductor Conference, 2004. CAS 2004 Proceedings. 2004 International Volume 2, Issue 4-6, 2004*, pp. 363 – 366.
- [11] J. Bogaerts, B. Dierickx, & R. Mertens: "Enhanced dark current generation in proton-irradiated CMOS active pixel sensors," *Nuclear Science, IEEE Transactions on*, Volume 49, Issue 3, Part 4, 2002, pp. 1513 – 1521.
- [12] J. Frenkel: "On pre-breakdown phenomena in insulators and electronic semi-conductors", *Physical Review*, Volume 54, 1938, pp. 647 – 648.
- [13] F. Wilkinson: "Chemical Kinetics and Reaction Mechanisms," Van Nostrand Reinhold Company, 1980, ISBN: 0-442-302248-7.
- [14] K. Gill, G. Hall & B. MacEvoy: "Bulk damage effects in irradiated silicon detectors due to clustered divacancies," *J. Appl. Phys.* Volume 82, Issue 1, 1997, pp. 126 – 136.